Food Chemistry 366 (2022) 130544

Contents lists available at ScienceDirect

Food Chemistry

journal homepage: www.elsevier.com/locate/foodchem

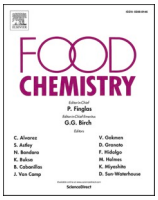

Separation of isomeric cereal-derived arabinoxylan-oligosaccharides by collision induced dissociation-travelling wave ion mobility spectrometry-tandem mass spectrometry (CID-TWIMS-MS/MS)

Minna Juvonen [a,*], Edwin Bakx [b], Henk Schols [b], Maija Tenkanen [a]

[a] Department of Food and Nutrition, University of Helsinki, P.O. Box 66, 00014 University of Helsinki, Finland
[b] Laboratory of Food Chemistry, Wageningen University & Research, Bornse Weilanden 9, 6708 WG Wageningen, Netherlands

ARTICLE INFO

Keywords:
Arabinoxylan
Oligosaccharides
Ion mobility spectrometry
Tandem mass spectrometry

ABSTRACT

The potential of travelling wave ion mobility spectroscopy in combination with collision induced dissociation tandem mass spectrometry (CID-TWIMS-MS/MS) to separate cereal-derived isomeric arabinoxylan-oligosaccharides (A)XOS was investigated. Three trisaccharide, four tetrasaccharide, and four pentasaccharide (A)XOS isomers were analyzed by positive and negative ionization TWIMS-MS and CID-TWIMS-MS/MS. The tri- and pentasaccharide isomers were distinguishable by the ATDs of the precursor ions. The CID-TWIMS-MS/MS could separate most of the isomeric fragment ions produced from tetra- and pentasaccharide (A)XOS. Finally, the base peak mobility spectrum is introduced as a practical tool for (A)XOS fingerprinting.

1. Introduction

Potential prebiotic and other health-related effects have increased interest in studying arabinoxylans (AXs), which are structural polysaccharides found in the cell wall of cereal grains. AXs in cereals form an integral part of human dietary fiber intake. The hydrolysis of AX by endoxylanases releases a mixture of arabinoxylooligosaccharides (AXOS) in addition to linear xylooligosaccharides (XOS).

Many studies have demonstrated that mass spectrometry, particularly tandem mass spectrometry (MS/MS), is a powerful tool for the characterization of oligosaccharide structures, including glycosidic linkage positions, branching, and sequences (Asam & Glish, 1997; Čmelík & Chmelík, 2010; Harvey, 2005; Hofmeister et al., 1991; Pfenninger et al., 2002; Quéméner et al., 2006). However, carbohydrates, such as (A)XOS, which are composed of the same mass monosaccharide residues often have the same *m/z* precursor ions and fragment to the same *m/z* fragment ions. Therefore, the ability of MS to separate and to identify isomeric structures of oligosaccharides in a mixture is limited, such as for the type of monosaccharide units (Juvonen et al., 2019). Our previous study (Juvonen et al., 2019) showed that although we could distinguish between all the studied (A)XOS oligosaccharides based on their different fragmentation patterns in the electrospray ionization (ESI) MS/MS spectra, the method could not characterize the structures with enough detail to reliably determine the structures of unknown samples.

Ion mobility spectrometry (IMS) is a technique that provides a new dimension for the separation of ions. In addition to MS, which separates ions by mass and charge, in IMS ions are also separated based on their shape and size. Ion mobility cell analytes are attracted through an inert gas (e.g., N_2 or He) by an electric field (Gabelica & Marklund, 2018). Analytes' travel time (drift time) through the cell is measured. The IMS analysis takes only milliseconds compared to chromatographic separations, which usually requires tens of minutes, so it is a rapid separation technique.

IMS coupled with MS (IMS-MS) has become of interest as a technique that can separate isomeric oligosaccharides. Gabryelski and Froese (2003) demonstrated that an in-house High-Field Asymmetric Waveform ion mobility spectrometer (FAIMS) coupled with MS was able to separate and to differentiate between anomers, linkage, and position isomers of disaccharides. Clowers et al. (2005) used the electrospray ionization-atmospheric pressure ion mobility-time of flight mass spectrometry (ESI-AP-IM-TOFMS) method for the separation of sodiated isobaric disaccharides and trisaccharides. Their group continued the study with the same technique and found that the method can separate isomeric glycosides and simple sugars (Dwivedi et al., 2007). Zhu et al. (2009) showed that the isomeric precursor ions of oligosaccharides and

* Corresponding author.
E-mail address: minna.juvonen@helsinki.fi (M. Juvonen).

https://doi.org/10.1016/j.foodchem.2021.130544
Received 4 September 2020; Received in revised form 12 June 2021; Accepted 4 July 2021
Available online 5 July 2021

oligosaccharide alditols could be analyzed by MS^n after separation by an ambient pressure ion mobility spectrometer. Fenn and McLean (2011) analyzed 31 different sodiated carbohydrates and their fragment ions using an in-house constructed uniform field MALDI-IM-MS. They also showed that pre- or post-IM fragmentation prior to MS can be advantageous when analyzing the positional and structural isomers by commercial travelling wave ion mobility spectroscopy (TWIMS). Pagel and Harvey (2013) presented the calibration protocol for TWIMS to convert drift times to collision cross section values (CCS) using complex sodiated glycans and CCS values measured by a drift tube IMS. Their study also showed improved resolution between the first-generation and second-generation TWIMS instruments. Leijdekkers et al. (2015) demonstrated that coupling TWIMS-MS to hydrophilic interaction liquid chromatography (HILIC) allows for analyzing complex pectic oligosaccharides in mixtures.

Negative ionization MS/MS has become a popular method for a structural analysis of oligosaccharides due to the more diagnostic MS/MS spectra than that of the positive ionization mode (Maina et al., 2013; Pfenninger et al., 2002; Quéméner et al., 2006). Some negative ionization IM-MS/MS methods have also been developed. Yamagaki and Sato (2009) performed analyses for isomeric oligosaccharides using negative-ion electrospray ionization ion mobility spectrometry combined with MS/MS. Harvey et al. (2013) reported promising results of TWIMS-MS/MS to separate negatively charged isomeric *N*-glycans. In 2014, Hofmann et al. implemented the Pagel and Harvey (2013) calibration method for negatively charged *N*-glycans and dextrans. Since then, hundreds of negatively charged *N*-glycans and their fragment ions have been analyzed (Hofmann et al., 2014).

Recently, researchers have shown that isomeric product ions can also be separated by new-generation IMS instruments. The benefit of using CID-TWIMS-MS/MS rather than TWIMS-MS/MS is that in addition to measuring the drift times of precursor ions, it also measures those of fragment ions as well. Both et al. (2014) found that with the second-generation TWIMS following MS/MS, it was possible to separate and to characterize certain C-glycans and glycopeptides in the positive ionization mode. Hofmann et al. (2015) performed a separation and structural analysis of connectivity and configurational trisaccharide isomers using TWIMS-MS/MS. Gaye et al. (2015) developed an IMS-CID-IMS-MS instrument that can distinguish between underivatized carbohydrate isomers based on the ion mobility distribution of lithiated fragment ions. Recently, Hofmann et al. (2017) presented using positive ionization CID-TWIMS-MS/MS for which Lewis and blood group epitope isomers with identical MS/MS spectra can be differentiated based on their fragment ion drift times.

In the present work, whether the TWIMS-MS technique would provide more information about the isomeric structures of AXOS than MS/MS was investigated. The aim of the study was to separate and to identify isomeric fragment ions produced from AXOS by TWIMS-MS. First, precursor ions were analyzed by TWIMS-MS using both positive and negative ionization. Second, the fragment ions from each sample were produced prior to the IM cell and analyzed by TWIMS-MS/MS. This method is abbreviated as CID-TWIMS-MS/MS.

2. Materials and methods

2.1. Samples

The AXOS samples (A^2X, A^3X, A^2XX, $A^{2+3}X$, $A^{2+3}XX$, and $D^{2,3}X$) were enzymatically released and isolated from cereal arabinoxylan as described previously (Pastell et al., 2008, 2009; Rantanen et al., 2007). Xylooligosaccharides (XOS: X_3, X_4, and X_5,) and three branched AXOS samples (XA^3XX, $XA^2XX + XA^3XX$, and $XA^{2+3}XX$) were purchased from Megazyme International (Bray, Ireland). The structures of the (A)XOS are presented in supplementary material (Fig. S1). AXOS abbreviations are according to Fáure et al. (2009). The samples were diluted in water in a concentration of 0.05 mg/mL.

2.2. ^{18}O-labelling of tetrasaccharide samples

The reducing end labelling with ^{18}O was performed according to Körner et al. (1999) for tetrasaccharide samples. 20 μg of dried sample were dissolved in 20 μL of ^{18}O-water (97 atom %, SigmaAldrich Chemie GmbH, Germany), containing 1.5 μL of formic acid (purity ≥ 99%, VWR Chemicals) in 250 mg of ^{18}O-water. Samples were incubated in room temperature for 24 h. Prior to analysis 1 μL of the reaction products were diluted in 100 μL of 50% acetonitrile to concentration 0.01 mg/mL and injected to ion source by syringe and infusion pump with a flow rate of 500 μL/hour.

2.3. TWIMS-MS and CID-TWIMS-MS/MS

TWIMS-MS and CID-TWIMS-MS/MS experiments were performed by Synapt G2-Si HDMS (Waters Corp, Manchester, UK) in both the positive and the negative ionization mode using an electrospray ionization source and direct infusion. In the TWIMS-MS analysis, the ionized analytes were first separated in the ion mobility cell and then analyzed using a TOF mass analyzer. In CID-TWIMS-MS/MS, the analytes were first fragmented in the trap cell using CID and then separated in the ion mobility cell. The *m/z* values of the product ions were then analyzed by TOF. The schematic presentations of both analyses are presented in the supplementary file (Fig. S2).

The ESI ion source parameters were: capillary voltage of 3.0 kV in the positive mode and 2.5 kV in the negative mode, sampling cone voltage of 40 V, source offset of 80 V, source temperature of 110 °C, desolvation temperature of 150 °C, cone gas flow of 50 L/h, desolvation gas flow of 600 L/h, and nebulizer gas flow of 6.0 bar. The MS instrument was calibrated with 0.5 mM sodium formate (Waters Corp) in the positive and negative ionization modes. Ion mobility was calibrated with a polyalanine mixture (Waters Corp) in positive and negative modes using the default parameters. Leucine enkephalin (Leu-Enk) was used for both the detector check and the CCS lock spray solution. The samples were analyzed in *m/z* 50–1200 mass ranges using the resolution mode. For CID-TWIMS-MS/MS, the transfer *T*-Wave velocity of 315 m/s was used. Nitrogen was used as the ion mobility gas and argon as the CID gas. The trap gas flow was 2.0 mL/min. Helium cell gas flow was 180 mL/min and IMS gas flow was 90 mL/min. Ion mobility calibration was created by ramping the IMS wave velocity between 300 and 1000 m/s in a mass range of *m/z* 50–1200. The wave velocity ramp 300–1000 m/s was also used in TWIMS-MS analysis for precursor ions (default method). For CID-TWIMS-MS/MS, the IMS wave velocity parameter was set to 800 m/s to separate the small product ions as well. IMS wave height was constant at 40 V for all measurements. For the positive ionization CID-TWIMS-MS/MS, the trap collision voltage was 40 V for trisaccharides, 50 V for tetrasaccharides, and 60 V for pentasaccharides. For the negative ionization mode trap collision, the voltage was 30 V for trisaccharides, 30 V for tetrasaccharides, and 35 V for pentasaccharides. The trim drift time velocity parameter was enabled for the default (calibration) method and disabled for CID-TWIMS-MS/MS. Prior to the analysis samples were diluted in an acetonitrile–water solution (4:1) with 0.1% of ammonium hydroxide for a final concentration of 10 μg/mL. Direct infusion was performed at 10–20 μL/min. For $[M + Cl]^-$ adduct formation, ammonium chloride was added to the sample solutions (10 μg/mL).

The $[M + Na]^+$, $[M-H]^-$, and $[M + Cl]^-$ precursor ions and their fragment ions were analyzed. The arrival time distribution (ATD) data were collected using MassLynx 4.1 software and analyzed using Unifi 1.8 software by drawing an extracted-ion mobility spectrum (EIM) and integrating the ATD peaks. The fragment ions were named according to Domon and Costello's (1988) nomenclature. An example of the fragment ion nomenclature is presented in Fig. 1.

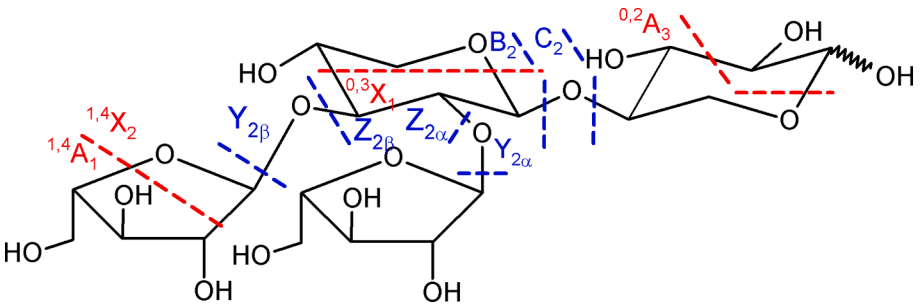

Fig. 1. Fictional example of Domon & Costellós fragment ion nomenclature. Superscripted numbers indicate the location of cross-ring bond cleavage in monosaccharide unit. Subscripted number indicates the location of the cleavage in the molecule. A-, B- and C-ions contain original non-reducing end and X-,Y- and Z-ions contain original reducing end. (Domon & Costello 1988).

3. Results and discussion

3.1. Potential of TWIMS-MS for the differentiation of (A)XOS isomers

First, the potential of TWIMS-MS to separate and differentiate the AXOS were studied. All 11 samples containing known XOS and AXOS oligosaccharides were analyzed by the TWIMS-MS using the default method. The ATDs of the oligosaccharides were measured as three different precursor ions. The ATDs in milliseconds (ms) of the $[M + Na]^+$, $[M-H]^-$, and $[M + Cl]^-$ precursor ions are presented in Table 1.

Trisaccharides. First, three (A)XOS trisaccharides (X_3, A^2X, and A^3X) were analyzed by TWIMS-MS in the positive ionization mode. The $[M + Na]^+$ adducts of A^2X and A^3X had very close ATDs—3.34 ms and 3.36 ms (Table 1)—and could not be differentiated from each other. X_3 had ATD 3.69 ms and about a 0.3 ms difference compared to A^2X and A^3X. Because the peak width was 0.4 ms, the peak resolution was only ~ 0.8. The difference in their ATDs should be at least 0.5 ms to achieve good (>1.0) peak resolution; however, for the structural analysis, a weaker peak resolution can often be adequate to distinguish between the isomeric ions. This may be possible until the resolution decreases to 0.5 (~0.2 ms difference between peaks) and the peaks are merged.

In the negative mode, almost the same ATDs were measured for all three trisaccharide $[M + Cl]^-$ ions: A^2X had 3.36 ms, A^3X had 3.42 ms, and X_3 had 3.47 ms (Table 1). In contrast, the ATD of A^2X was notably lower than the others as $[M-H]^-$ ions. A^2X was observed to be the fastest in all tested adduct ion forms. The results demonstrate that all these trisaccharide samples can be distinguished between by TWIMS-MS when analyzing the ATDs of both $[M-H]^-$ and $[M + Na]^+$ ions;

Table 1
ATDs of (A)XOS precursor ions in TWIMS-MS. $[M + Na]^+$, $[M-H]^-$, and $[M + Cl]^-$ ions. DP = degree of polymerization, *m/z* = mass-to-charge ratio, ATD = arrival time distributions, parentheses = minor peak. AXOS abbreviations according to Fauré et al. 2009.

		$[M+Na]^+$			$[M-H]^-$			$[M+Cl]^-$		
(A)XOS	DP	*m/z*	ATD (ms)		*m/z*	ATD (ms)		*m/z*	ATD (ms)	
A^2X	3	437	3.34	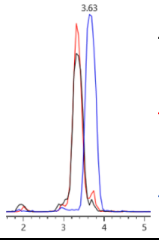	413	3.09	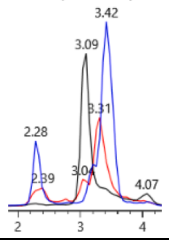	449	3.36	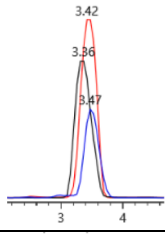
A^3X	3	437	3.36		413	3.31		449	3.42	
X_3	3	437	3.69		413	3.42 (2.28)		449	3.47	
A^2XX	4	569	4.56, (4.94)	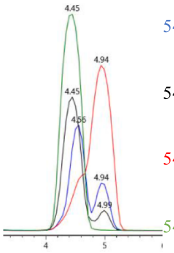	545	4.01	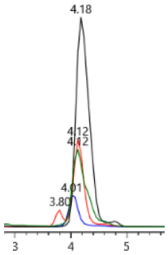	581	4.39	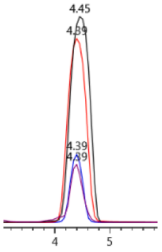
$A^{2+3}X$	4	569	4.45		545	4.18		581	4.45	
$D^{2,3}X$	4	569	4.45, (4.99)		545	4.12, (3.80)		581	4.39	
X_4	4	569	4.94		545	4.12		581	4.39	
$A^{2+3}XX$	5	701	5.64	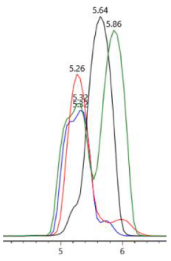	677	4.77	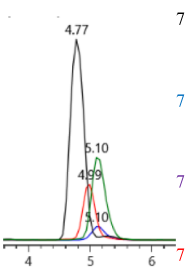	713	5.21	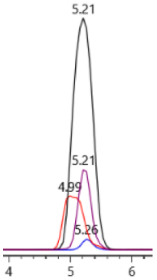
XA^2XX +XA^3XX	5	701	5.86, 5.32		677	5.10		713	5.26	
XA^3XX	5	701	5.32		677	5.10		713	5.21	
X_5	5	701	5.26		677	4.99		713	4.99	

however, if all three trisaccharides are analyzed as a mixture, chromatographic separation is needed in addition to TWIMS-MS.

Tetrasaccharides. The four analyzed (A)XOS tetrasaccharide isomers were one branched ($A^{2+3}X$) and three linear (A^2XX, $D^{2,3}X$ and X_4) (A)XOS. Surprisingly, using TWIMS-MS, identical ATDs (4.45 ms) of $[M + Na]^+$ adduct ions were measured for the branched $A^{2+3}X$ and the linear $D^{2,3}X$ (Table 1). The ATD of A^2XX was also very close, being only 0.1 ms apart from the previous, but X_4 had a clearly lower ATD: 4.94 ms. The branched isomer were expected to have more compact structure than linear isomers and therefore travel faster, similarly as seen with LNFP2 and LNFP1 pentasaccharides separated in Fenn & McLean's (2011) study. However, the conformation of gas-phase ion is not always so predictable, and for example Hofmann et al. 2017 study showed that two isomeric branched trisaccharide fragments, which had very similar structures, were separated nearly by baseline and the other one had ATD close to their linear isomers. In the negative mode, all four analytes had very close ATDs. As $[M-H]^-$ ions, their ATDs were between 4.07 ms and 4.18 ms. As $[M + Cl]^-$ ions, the ATD of $A^{2+3}X$ was 4.45 ms, and all three other samples had a ATD of 4.39 ms. This means that the TWIMS-MS method did not separate the AXOS tetrasaccharide isomers sufficiently enough to recognize them individually when present in a mixture. Only X_4, which is XOS, could be differentiated from the Ara-substituted AXOS using TWIMS-MS and the positive ionization mode.

Pentasaccharides. The (A)XOS pentasaccharides consisted of three branched AXOS samples ($A^{2+3}XX$, XA^3XX, and a mixture of XA^2XX and XA^3XX) and one linear XOS (X_5). All pentasaccharides had different main ATDs as $[M + Na]^+$ ions based on the TWIMS-MS analysis (Table 1), which means they can be differentiated from each other. The main ATD of X_5 was 5.26 ms, XA^3XX was 5.32 ms and $A^{2+3}XX$ was 5.64 ms. XA^3XX was split to two-headed peak. This might be caused by the XA^3XX having two different conformations as $[M + Na]^+$ precursor ion. The metal adducts are known to affect to the conformation of oligosaccharides, and especially larger oligosaccharides with five or more monosaccharide residues may have several dominant conformers (Fukui et al., 2006). It was also noted that the precursor ion peaks in the mixture of XA^2XX and XA^3XX were visibly separated (5.86 ms and 5.32. ms) and had good peak resolution. The mixture was analyzed by HILIC-IM-MS, which showed that the ATM peak of XA^2XX was separated from XA^3XX peak and confirmed the ATM of XA^2XX to be 5.86 ms (Fig. S3). For the negative ionization TWIMS-MS, all four samples had ATDs close to each other. ATDs as $[M-H]^-$ ions were 4.77 ms for $A^{2+3}XX$, 5.10 ms for mixture of XA^2XX and XA^3XX, 5.10 ms for XA^3XX, and 4.99 ms for X_5. The ATDs as $[M + Cl]^-$ ions were 5.21 ms for $A^{2+3}XX$ and XA^3XX, 5.26 ms for $XA^2XX + XA^3XX$, and 4.99 ms for X_5.

Interestingly, $A^{2+3}XX$ had the smallest ATD as a $[M-H]^-$ ion, but X_5 had smallest ATD as a $[M + Cl]^-$ and a $[M + Na]^+$ ions. This means that formation of adduct ions have changed the conformation of molecules. Struwe et al. (2016) suggested that metal ion adducts make oligosaccharides more compact. They found that certain structural isomers of human milk oligosaccharides can be separated by IM-MS as deprotonated ions but not as protonated species or sodium/chloride adducts. We also observed that different adducts and deprotonated ions of isomeric (A)XOS separated differently; however, in contrast to human milk glycans, the studied isomeric (A)XOS were best separated as sodium adduct forms.

3.2. Differentiation of isomeric glycosidic bond fragment ions by CID-TWIMS-MS/MS

Next, the ability of CID-TWIMS-MS/MS to identify the isomeric (A)XOS samples and to differentiate between the isomeric fragment ions was studied. The $[M + Na]^+$ and $[M + Cl]^-$ precursor ions were fragmented by CID-TWIMS-MS/MS, and the extract ion mobility spectra (EIMs) of each product ion were analyzed. The fragment ions ATDs were averaged from the three measurements of 30 s of data collection. The standard deviation of ATDs within triplicates varied between 0.00 ms and 0.04 ms. The standard deviation was smaller in the abundant peaks. For example, the standard deviations of the base peaks were between 0.00 ms and 0.02 ms, and the minor peaks (marked in Table 2 and Table 3 with parentheses), which had a poor ion intensity level and often an asymmetric peak shape, had a standard deviation of 0.01 ms − 0.04 ms.

$[M + Na]^+$ glycosidic bond fragment ions. The ATDs of $[M + Na]^+$ fragment ions were determined by CID-TWIMS-MS/MS and are presented in Table 2. It was observed that the isomeric disaccharide fragment ions at *m/z* 305 could not be differentiated from each other. All samples had only one ATD peak for *m/z* 305 between 3.33 and 3.35 ms. It is known that in positive ionization, the B- and Y-type fragmentation is favored of over C- and Z-type fragmentation (Hofmeister et al., 1991) and therefore it was considered if all of the *m/z* 305 peaks were Y-ions and in fact represent an xylobiose fragment ion from the reducing end of samples; however, because the ATDs of *m/z* 287 ions, which are most likely B-type disaccharide fragment ions from the non-reducing end, only slightly varied (<0.1 ms), it was clear that the reliable differentiation of isomeric disaccharide structures (Ara-Xyl, Xyl-Ara vs. X_2) is impossible with this method.

The (A)XOS trisaccharides formed $[M + Na]^+$ precursor ions at *m/z* 437. The CID-TWIMS-MS/MS measured the ATDs of A^3X, A^2X, and X_3 at 4.69 ms, 4.70 ms, and 5.16 ms, respectively (Table 2). When compared to ATDs measured with TWIMS-MS (Table 1), the X_3 was, now due to used higher wave velocity, more apart from AXOS and was clearly distinguishable from its arabinose-containing isomers. The ions at *m/z* 437 in the MS/MS of tetrasaccharides and pentasaccharides were either C- or Y-type glycosidic bond fragment ions formed of three pentose residues. The *m/z* 437 with a 5.17 ms ATD peak was detected at the EIM of X_4, A^2XX, and all pentasaccharide samples. The 5.17 ms ATD peak in X_4 and A^2XX were confirmed by reducing-end ^{18}O-labelling (data not shown) to be Y-type ion, which means a xylotriose (X_3) structure. The 5.17 ms ATD was not present in the EIM of $A^{2+3}X$ or $D^{2,3}X$, which is logical because they cannot fragment to X_3 ions. $D^{2,3}X$ had two ATDs for *m/z* 437 ions: a major peak at 4.73 ms and a minor peak at 4.99 ms (Table 2). The ion at ATD 4.73 ms was confirmed by the reducing end ^{18}O-labelling (data not shown) to be the Y-ion, which had the structure of A^3X. The small peak at the 4.99 ms was most likely from impurity in the sample.

The $A^{2+3}X$, A^2XX, $A^{2+3}XX$, XA^2XX, and XA^3XX samples had arabinose attached to the xylose backbone, and all had the *m/z* 437 peak at the 4.67–4.75 ms ATDs, similar to the A^3X and A^2X precursor ions. The fragment ions with an A^3X or A^2X structure indicated that $A^{2+3}XX$, XA^2XX, and XA^3XX had to fragment from both the reducing and the non-reducing ends of the molecule (Y- and C- type co-fragmentation). Another possibility is that branched XA^2, XA^3, and A^{2+3} fragments had the same ATD as A^3X and A^2X.

The (A)XOS tetrasaccharides formed $[M + Na]^+$ precursor ions at *m/z* 569 (Table 2). Similar to what was observed with trisaccharides, the X_4 precursor travelled in TWIMS notably slower compared to other tetrasaccharides. The precursor ion of X_4 had a split ATD peak at 6.84 ms and 7.22 ms according to the CID-TWIMS-MS/MS. 6.39 ms for $A^{2+3}X$, 6.55 ms for A^2XX (also a minor peak at 6.15 ms), and 6.39 ms for $D^{2,3}X$ were measured for other tetrasaccharides. All the pentasaccharide samples had different ATDs for the main *m/z* 569 fragment ion. The EIM of X_5 had ATDs 6.69 ms and 7.20 ms for the *m/z* 569 ion, which are very close to the X_4 precursor ion ATD, as expected. The ATD of $A^{2+3}XX$'s product ion at *m/z* 569 was 6.47 ms. It was also observed that $A^{2+3}XX$ was the only pentasaccharide sample lacking the 7.2 ms peak for *m/z* 569, which is understandable because the $A^{2+3}XX$ cannot fragment to an X_4 ion. When $A^{2+3}XX$ loses one pentose residue, it can form a C-ion ($A^{2+3}X$) or two types of Y-ions: A^3XX or A^2XX. All branched tetrasaccharides also had a ATD peak near 6.1 ms, but this was not present in the mobility spectrum of unbranched X_4. A small ATD indicates that the ion has a more compact structure than the other isomers. The mixture of the XA^2XX and XA^3XX sample had 6.69 ms as the major peak at *m/z* 569 and

Table 2
ATDs of precursor and fragment ions measured by CID-TWIMS-MS/MS. Positive mode $[M + Na]^+$ adducts. Underline = base peak, parentheses = minor peak, P = pentose residue, Da = dalton.

Sample	CID fragment ions $[M-X+Na]^+$ (*m/z*) and their ATDs (ms)													
	701	683	641	611	569	551	509	479	437	419	377	347	305	287
Tri-saccharides									$[M+Na]^+$ Precursor	$[M-18Da+Na]^+$	$[M-60Da+Na]^+$	$[M-90Da+Na]^+$	$[M-P+Na]^+$	$[M-P-18Da+Na]^+$
A^2X									4.69	4.58	4.03	3.75	3.33	3.20
A^3X									4.70	4.64	4.05	3.77	3.33	3.24
X_3									5.16	4.97	4.43	3.90	3.36	3.13
Tetra-saccharides					$[M+Na]^+$ Precursor	$[M-18Da+Na]^+$	$[M-60Da+Na]^+$	$[M-90Da+Na]^+$	$[M-P+Na]^+$	$[M-P-18Da+Na]^+$	$[M-P-60Da+Na]^+$	$[M-P-90Da+Na]^+$	$[M-2P+Na]^+$	$[M-2P-18Da+Na]^+$
$A^{2+3}X$					6.39	6.09	5.67	5.32	4.67	4.59	4.03	3.77	3.33	3.21
A^2XX					6.55, (6.15)	6.12	5.66	5.34	(4.69),5.17	4.45,(4.85)	4.04,4.45	–	3.34	3.14
$D^{2,3}X$					6.39	6.15	5.70	5.41	4.73,(4.99)	4.79	4.04	3.76	3.35	3.23
X_4					(6.84,7.22)	–	6.24	5.85	5.17	4.85	4.43	3.88	3.34	3.14
Penta-saccharides	$[M+Na]^+$ Precursor	$[M-18Da+Na]^+$	$[M-60Da+Na]^+$	$[M-90Da+Na]^+$	$[M-P+Na]^+$	$[M-P-18Da+Na]^+$	$[M-P-60Da+Na]^+$	$[M-P-90Da+Na]^+$	$[M-2P+Na]^+$	$[M-2P-18Da+Na]^+$	$[M-2P-60Da+Na]^+$	$[M-2P-90Da+Na]^+$	$[M-3P+Na]^+$	$[M-3P-18Da+Na]^+$
$A^{2+3}XX$	8.50, (7.77)	7.92	7.51	7.16	6.47,(6.10)	6.10	5.31,5.64	5.36	4.69,(5.16)	4.49	(4.03),4.42	3.82	3.34	3.17
XA^2XX $(+XA^3XX)$	(7.45,7.85,) 8.90	(7.26,7.73),8.36	(7.02),7.90	7.51	(6.04,)6.69, (7.22)	6.44	(5.31,5.66),6.23	5.38,5.85	4.75,5.17	4.55,(4.82)	(4.03),4.42	3.82	3.33	3.11
XA^3XX	7.53,7.86	7.24,7.75	7.04	7.41	6.10,6.56,7.24	6.12,6.41	5.32,(5.84,)6.24	5.42,5.86	4.73,5.16	4.50,4.82	4.02,4.42	–	3.33	3.23
X_5	7.78	7.45	6.62	7.49,8.16	(6.69),7.20	6.63,6.93	(5.72,)6.24	(5.35),5.85	(4.75),5.16	4.85	(4.06),4.42	3.88	3.34	3.14

Table 3
ATDs of precursor and fragment ions measured by CID-TWIMS-MS/MS. Negative mode $[M + Cl]^-$ adducts. Underline = base peak, parentheses = minor peak, P = pentose residue, Da = dalton.

Sample	Precursor	CID fragment ions $[M-X-H]^-$ and their drift times														
	$[M+Cl]^-$	677	617	599	587	545	527	485	467	455	413	395	353	335	323	263
Tri-saccharides	449										$[M-H]^-$		$[M-60Da-H]^-$	$[M-78Da-H]^-$	$[M-90Da-H]^-$	$[M-H-P-18Da]^-$
A^2X	4.65										–		3.97	3.73	3.59	2.88
A^3X	4.80										–		4.00	3.73	3.59	2.96
X_3	4.83										4.74		3.97	3.76	3.60	2.86
Tetra-saccharides	581					$[M-H]^-$	$[M-18Da-H]^-$	$[M-60Da-H]^-$	$[M-78Da-H]^-$	$[M-90Da-H]^-$	$[M-P-H]^-$	$[M-P-18Da-H]^-$	$[M-P-60Da-H]^-$	$[M-P-78Da-H]^-$	$[M-P-90Da-H]^-$	$[M-2P-18Da-H]^-$
$A^{2+3}X$	6.40					6.07	–	5.37	5.15	4.99	4.45	4.51	3.96	3.72	3.58	2.95
A^2XX	6.29					5.72	–	5.18	5.33,(5.01)	5.00	4.31	(4.14),4.40	–	3.74	3.60	2.87
$D^{2,3}X$	6.29					(5.32), 5.93	5.73	5.20	4.99,(5.56)	4.81	4.32,(4.74)	4.52	3.97	3.72	3.59	2.95
X_4	6.18					(5.45),5.74	–	5.84	5.64	5.44	(4.30),4.68	4.50	3.97	3.76	3.60	2.87
Penta-saccharides	713	$[M-H]^-$	$[M-60Da-H]^-$	$[M-78Da-H]^-$	$[M-90Da-H]^-$	$[M-P-H]^-$	$[M-H-P-18Da]^-$	$[M-P-60Da-H]^-$	$[M-P-78Da-H]^-$	$[M-P-90Da-H]^-$	$[M-2P-H]^-$	$[M-2P-18Da-H]^-$	$[M-2P-60Da-H]^-$	$[M-2P-78Da-H]^-$	$[M-2P-90Da-H]^-$	$[M-3P-18Da-H]^-$
$A^{2+3}XX$	7.60	6.87	7.44	7.08	6.95	6.09	5.92	5.34, (5.85)	5.16,5.60	5.01,5.43	4.45	4.49	–	3.73	3.59	2.92
XA^2XX $(+XA^3XX)$	7.66	7.43	7.76	7.43	7.22	(5.67),6.47	6.15	5.65	5.48	(5.01),5.38	4.74	(4.24),4.49	3.98	3.74	3.60	2.87
XA^3XX	7.71	7.66	7.66	7.37	7.15	(5.80),6.31	6.11	5.50	5.22,(5.63)	(5.04),5.46	–	(4.24),4.51	–	3.75	3.61	2.88
X_5	7.20	7.20	6.56	6.67	6.39	5.75	6.34	5.82	5.63	5.44	(4.31),4.65	4.50	3.98	3.76	3.61	2.87

two minor peaks at 6.04 ms and 7.22 ms. When compared to the *m/z* 569 EIM of XA^3XX, which had three peaks (6.10 ms, 6.56 ms, and 7.24 ms) with almost the same intensity, it can be assumed that the 6.69 ms peak was the *m/z* 569 ion that fragmented from XA^2XX.

Few studies have been conducted to measure the ATDs of glycosidic fragment ions using the CID-TWIMS-MS/MS method. Both et al. (2014) differentiated monosaccharide fragment ions from epimeric disaccharides by positive ionization TWIMS; however, contrary to our results, almost all the disaccharide ions were distinguishable in the study of Both et al. (2014). The reason for the different results may be structural differences in the samples: *N*-linked glycan disaccharides are composed of two monomers (hexoses and *N*-acetylglucosamines) with different masses, whereas (A)XOS are composed of pentoses of the same mass. Both et al. (2014) also increased the traveling wave speed to 1200 m/s (ours 800 m/s). Hofmann et al. (2017) made similar observations on di- and oligosaccharide fragment ions. They found that the $[M + Na]^+$ ion mobility spectra of precursor and fragment ions of Lewis and blood group oligosaccharides are unique and systemically differentiate between isomers. Even the previously challenging indistinguishable structures which had identical tandem mass spectra were separated by CID-TWIMS-MS/MS. These results suggest that the CID-TWIMS-MS/MS method's ability to differentiate between the isomeric disaccharide-sized fragment ions of (A)XOS should be further studied.

$[M-H]^-$ glycosidic bond fragment ions from $[M + Cl]^-$ precursors. Various studies have reported that in MS/MS, the precursors with anion adducts mainly fragment to deprotonated product ions (Harvey, 2005; Juvonen et al., 2019). Because both $[M + Cl]^-$ and $[M-H]^-$ fragment to the same deprotonated ions, the results on only one are presented here (Table 3). As the $[M + Cl]^-$ precursors had a higher ionization intensity level than the deprotonated precursors, they were chosen for CID-TWIMS-MS/MS. The qTOF-MS/MS spectra were observed to have much less C-ions than in our previous study (Juvonen et al., 2019), which was carried out using an ion trap mass spectrometer. Abundant C-ions would be useful for the analysis of the non-reducing end.

Disaccharide-sized glycosidic bond fragment ions were formed only at *m/z* 263, which means they were either B- or Z-ions. All samples had only one ATD for the *m/z* 263 ions, and the ATDs were between 2.87 ms and 2.96 ms (Table 3). All ATDs being so close to each other indicates that all fragments were either Z-ions (X_2-H_2O) or that the method cannot differentiate isomeric Ara-Xyl, Xyl-Ara, and xylobiose structures either in the negative or in the positive ionization mode.

Fragment ions at *m/z* 413 were deprotonated trisaccharide ions. Because there were differences between the ATDs of $[M-H]^-$ precursors, it was assumed that the *m/z* 413 fragment ions formed from other oligosaccharides could be identified if they have the same structure as deprotonated trisaccharides. It was found that X_3 had an *m/z* 413 peak at 4.74 ms when analyzed using CID-TWIMS-MS/MS (Table 3). Unfortunately, the A^2X and A^3X trisaccharides did not form *m/z* 413 fragment ions from the $[M + Cl]^-$ precursor using CID-TWIMS-MS/MS; however, from the $[M-H]^-$ precursor ion mobility spectra measured with the same parameters but recorded using TWIMS-MS, it was observed that all trisaccharide samples had different ATDs: 4.23 ms for A^2X, 4.50 ms for A^3X, and 4.67 for X_4. Similar differentiations in the ATDs of *m/z* 413 fragments were observed for tetra- and pentasaccharide $[M + Cl]^-$ CID-TWIMS-MS/MS ion mobility spectra. The main *m/z* 413 peak in the EIM of X_4 was measured to have a 4.68 ms ATD. The $D^{2,3}X$ had a minor peak at 4.74 ms, indicating a xylose backbone consisting of a Y_3 fragment ion. $A^{2+3}X$ and $A^{2+3}XX$ had the same ATD, 4.45.ms, for the *m/z* 413 ion. These *m/z* 413 peaks are likely A^{2+3} fragment ions formed by C-type fragmentation, but based on the ATD, they could also be A^3X fragment ions. The *m/z* 413 fragment ions from A^2XX and $D^{2,3}X$ also had very close ATDs: 4.31 ms and 4.32 ms, respectively. These ATDs being so close to trisaccharide A^2X's ATD implies a C-type fragmentation. Furthermore, close ATDs also indicate that A^2X and $D^{2,3}$ fragment ions cannot be differentiated from each other in the negative mode. Similar observations were made for pentasaccharides' EIMs. $A^{2+3}XX$ had a ATD of 4.45 ms for *m/z* 413, which is the same as that of $A^{2+3}X$ and supports the C_3-ion theory (formation of the A^{2+3} ion). XA^2XX had an *m/z* 413 peak at 4.74 ms, which indicates that it may be a xylotriose-structured fragment Y_3. X_5 had an *m/z* 413 at 4.65 ms, which is close to 4.68 ms measured from X_4. Interestingly, both also had minor *m/z* 413 peaks at 4.3 ms, which could have been due to impurities or ions with other conformations.

The tetrasaccharide-sized deprotonated fragment ion at *m/z* 545 had a ATD of 5.74 ms for X_4 and X_5. A^2XX had a very close ATD (5.72 ms) to them. The *m/z* 545 ion from $A^{2,3}X$ and $A^{2,3}XX$ had close ATDs, 6.07 and 6.09 ms, which suggests the C-ion fragmentation of $A^{2,3}XX$ and the formation of an $A^{2,3}X$ structured ion. $D^{2,3}X$ had two ATDs for the *m/z* 545 ion: minor at 5.32 ms and major at 5.93 ms. Branched XA^3XX also had two peaks: a minor peak at 5.80 ms and a major peak at 6.30 ms, most likely from the Y-ion (X_4) and the C-ion (XA^3X), respectively.

Summary of precursor and glycosidic bond cleavage ions and ATDs. Table 4 presents a summary of the (A)XOS precursor ions and the assumed C- or Y-type fragment ions, their *m/z*, and the measured ATDs of both negative and positive CID-TWIMS-MS/MS. The results indicate that the ATDs can be used for the identification of isomeric (A)XOS fragment ions. Because the negative and positive mode can separate different ions, the structural analysis of the unknown sample by CID-TWIMS-MS/MS should be performed with both ionization modes. Nonetheless, it should be noted that some assumptions when identifying the C- and Y-type fragments were made, and therefore, before using the method, the C- and Y-ions should be distinguishable, such as with a derivatization of the reducing end with ^{18}O-labelling (Hofmeister et al., 1991). Also, the reducing end labelling with 2-AB or some other derivatives would help to separate the C- and Y-ions, but in that case the Y-ion would be chemically different than the underivatized ion.

Table 4
Structures of (A)XOS precursor and fragment ions, their *m/z* and ATDs from CID-TWIMS-MS/MS. [a] ATD from TWIMS-MS, [b] ATD uncertain, sample is a mixture, [c] ATD uncertain, identification based on assumption of C-ion, [d]ATD uncertain, identification based on assumption of Y-ion, parentheses = minor peak.

		$[M + Na]^+$		$[M-H]^-$	
Structure	Ion	*m/z*	ATD (ms)	*m/z*	ATD (ms)
A^2X	precursor	437	4.7	413	4.3
A^3X	precursor	437	4.7	413	4.5[a]
$D^{2,3}$	fragment	437		413	4.3[c]
X_3	precursor	437	5.2	413	4.7
A^2XX	precursor	569	6.6	545	5.7
A^3XX	fragment	569	6.1[d]	545	
$A^{2+3}X$	precursor	569	6.4	545	6.1
$D^{2,3}X$	precursor	569	6.4	545	5.9
XA^2X	fragment	569		545	6.5[b]
XA^3X	fragment	569		545	6.3[c]
X_4	precursor	569	(6.7–6.8),7.2	545	5.7–5.8
$A^{2+3}XX$	precursor	701	8.5	677	6.9
XA^2XX	precursor	701	8.9	677	7.4[b]
XA^3XX	precursor	701	7.5,7.9	677	7.7
X_5	precursor	701	7.8	677	7.2

3.3. Differentiation of isomeric cross-ring cleavage fragment ions by CID-TWIMS-MS/MS

Usually, cross-ring ions are formed from the reducing end of the oligosaccharide molecule via a retro-aldol reaction (Hofmeister et al., 1991). They can also be formed from the new reducing end that has been formed in the mass spectrometer after C-type glycosidic bond fragmentation (Maina et al., 2013). Cross-ring cleavage ions have been found to be a diagnostic for the determination of the linkage positions from di- and oligosaccharides (Hofmeister et al., 1991; Juvonen et al., 2019).

In the present study, the ATDs of cross-ring ions from isomeric AXOS were analyzed by CID-TWIMS-MS/MS to determine whether they can

differentiate the isomeric ions.

[M + Na]$^+$ cross-ring fragment ions. The (A)XOS have a (1 → 4)-linked xylan backbone at the reducing-end and were fragmented in the positive ionization mode to abundant ^{0,2}A and minor ^{2,4}A ions by losses of 60 Da and 90 Da neutral fragments, respectively. The cross-ring fragment ions formed by a loss of 60 Da (^{0,2}A-ions) from the oligomers were found to have notably different ATDs for arabinose-substituted fragments compared to xylan backbone fragments (Table 2). The cross-ring fragment ion *m/z* 377 at A^{2}X EIM had a ATD 4.03 ms, A^{3}X had 4.05 ms, and X$_3$ had 4.43 ms. It was also observed that tetrasaccharides, which did not have a xylotriose backbone, had only one *m/z* 377 peak near 4 ms: A^{2+3}X had *m/z* 377 at 4.03 ms and D^{2,3}X had *m/z* 377 at 4.04 ms. In contrast, X$_4$, which is formed from (1 → 4)-linked xylopyranosyl units, had only one ATD at 4.43 ms. Some (A)XOS formed both ATD peaks for *m/z* 377. A^{2}XX showed two peaks at 4.04 ms and at 4.45 ms, which had similar intensities. This was also observed for XA^{3}XX (4.02 ms and 4.42 ms). Pentasaccharides A^{2+3}XX, XA^{2}XX + XA^{3}XX, and X$_5$ all had 4.42 ms as the main peak and a minor peak near 4 ms. The ions with a 4.42 ms

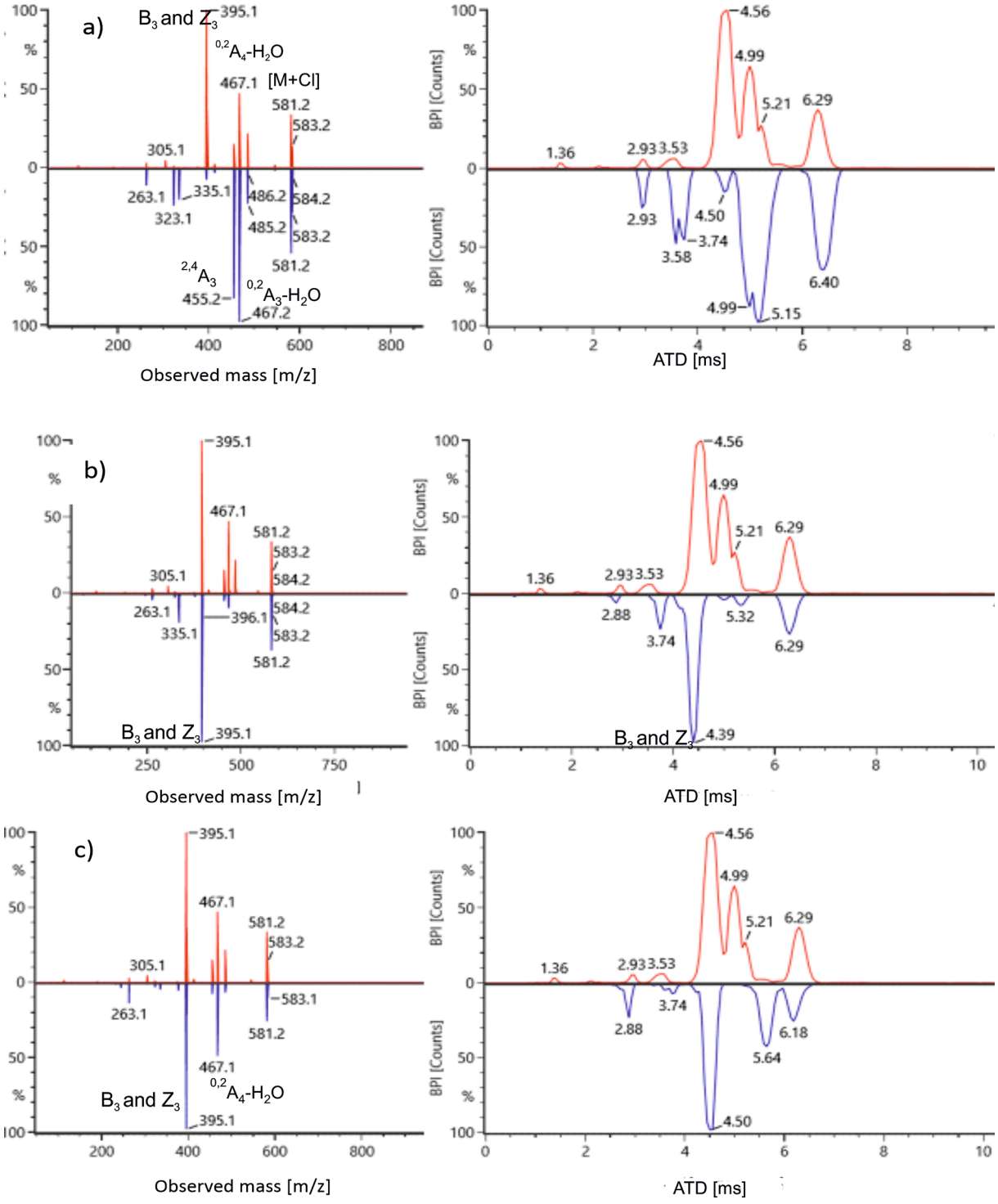

Fig. 2. Comparison of tetrasaccharide (A)XOS by CID-TWIMS-MS/MS. Negative [M + Cl]$^-$ base peak MS/MS spectra (left) and BPMs (right). a) D^{2,3}X (above) and A^{2+3}X (below), b) D^{2,3}X (above and A^{2}XX (below), c) D^{2,3}X (above) and X$_4$ (below).

ATD must have been formed by a combination of Y- and A-type co-fragmentations to have the structure of X_3. The *m/z* 377 ions near a 4 ms ATD seemed to contain arabinose substituents and could have been formed by either a C- and A-type fragmentation or a Y- and A-type fragmentation. The minor peak at 4.06 at X_5 EIM could have been an impurity.

The cross-ring ion at *m/z* 509, which fragmented from X_4, had clearly different ATDs (6.24 ms) compared to the cross-ring ions from arabinose-substituted tetrasaccharides: 5.67 ms, 5.66 ms, and 5.70 ms ($A^{2+3}X$, A^2XX, and $D^{2,3}X$, respectively). Pentasaccharides XA^2XX + XA^3XX and X_5 had *m/z* 509 also at 6.24 ms (6.23 ms for XA^2XX + XA^3XX). $A^{2+3}XX$ did not have a peak but instead an *m/z* 509, which separated into 5.31 ms and 5.64 ms peaks. The latter was likely formed by a combination of C- and A-type co-fragmentation ($A^{2+3}X$-60 Da ion) or a combination of Y- and A-type co-fragmentation (A^2XX-60 Da ion). The peak at 5.31 ms could have been a combination of Y- and A-type fragmentation and could have formed the A^3XX-ion because the same peak (5.32 ms) was observed at the EIM of XA^3XX.

The ^{0,2}A-type cross-ring fragmentation from pentasaccharides by a loss of 60 Da formed *m/z* 641 ions. These ions were found to have different ATDs for all isomers. The *m/z* 641 ions of X_5 were the fastest with a ATD 6.62 ms, followed by XA^3XX at 7.04 ms, $A^{2+3}XX$ at 7.51 ms, and XA^2XX + XA^3XX at 7.90 ms and 7.02 ms.

$[M—H]^-$ cross-ring fragment ions. In the negative mode, the cross-ring fragmentation of (A)XOS was formed by a loss of 60 Da, 78 Da, and 90 Da neutrals. The abundance of each fragment ion depends on the position of the glycosidic linkage (Juvonen et al., 2019). The EIMs showed that the cross-ring ions formed from three trisaccharide isomers, A^2X, A^3X and X_3, were not separated and had very close ATDs (Table 3: *m/z* 323, *m/z* 335, and *m/z* 353). At the tetrasaccharide EIMs, the X_4 cross-ring ions at *m/z* 485, *m/z* 467, and *m/z* 455 were found to have lower ATDs compared to the AXOS samples. ^{0,2}A ions formed by a loss of 60 Da neutral at *m/z* 485 had very close ATDs for A^2XX and $D^{2,3}X$ (5.18 ms and 5.20 ms, respectively); however, the ions formed by 78 Da and 90 Da cross-ring fragmentation had clearly different ATDs: A^2XX 5.33 ms and 5.00 ms and $D^{2,3}X$ 4.99 ms and 4.81 ms, respectively. On the other hand, oligomer $A^{2,3}X$ showed almost the same ATD for *m/z* 455 as A^2XX (4.99 ms) but was differentiated by other cross-ring ions at *m/z* 485 (5.37 ms) and at *m/z* 467 (5.15 ms). The similarities in these cross-ring ions' ATDs were observed in pentasaccharides EIMs. For example, $A^{2+3}XX$ formed a major peak at 5.34 ms (similar to $A^{2+3}X$) and a minor peak at 5.85 ms (similarly to X_4) from *m/z* 485 and peaks at 5.15 ms and 5.60 ms from *m/z* 467. Linear X_5 logically had the same ATDs for *m/z* 485, *m/z* 467, and *m/z* 455 as X_4 at 5.82 ms, 5.63 ms, and 5.44 ms, respectively. Interestingly, XA^3XX and XA^2XX + XA^3XX formed cross-ring ions, which had ATDs between the X_4 and $A^{2+3}X$ times. This suggests that these cross-ring ions were formed from C-ion structured XA^3X and XA^2X. Unfortunately, there were no XA^3X or XA^2X samples to test this theory.

3.4. Fingerprinting (A)XOS samples with base peak ion mobility and MS/MS spectra

The base peak mobility spectra (BPMs) of isomeric tetrasaccharides appeared to have potential for oligomer characterization and the usability of BPM was studied in more detail. The positive ionization MS/MS spectra and BPMs are presented in the supplementary file (Fig. S4). In Fig. S4, the MS/MS spectra (on the left) and BPM (on the right) of $D^{2,3}X$ have been compared to other DP4 isomers: $A^{2+3}X$ (Fig. S4a), A^2XX (Fig. S4b) and X_4 (Fig. S4c). It can be seen that all had fragmented to the same *m/z* ions in the positive MS/MS, but some exceptions were found. The *m/z* 245 was absent in the spectrum of $A^{2+3}X$ and A^2XX. Although MS/MS spectra of tetrasaccharide isomers had many fragment ions with the same *m/z*, the BPM on the right shows that they had differences in ATDs and the isomers could be distinguished from each other.

Fig. 2 presents the negative ion MS/MS spectra and BPMs of $D^{2,3}X$ (above) compared to other tetrasaccharide AXOS ions (below). In Fig. 2a, the negative ion MS/MS and the BPMs of $D^{2,3}X$ (above) are compared to $A^{2+3}X$ (below). Their MS/MS spectra show that the fragment ions had the same *m/z*- ratios but differed in ion abundancies, which can clearly be observed based on their BPM profiles. The most abundant peak in the negative ion BPM of $D^{2,3}X$ was at 4.56 ms, and that of $A^{2+3}X$ was at 5.15 ms. The $D^{2,3}X$ and A^2XX had identical ATDs for the precursor ion, but their fragment ion MS/MS spectra and BPMs showed clear differences (Fig. 2b). For example, $D^{2,3}X$ had a peak at 4.99 ms, and A^2XX had a peak at 3.74 ms. In Fig. 2c, the MS/MS spectra and BPMs of $D^{2,3}X$ (above) and X_4 (below) are compared. Although their MS/MS spectra had many fragment ions with the same *m/z*, the BPMs had differences in ATDs (Fig. 2c, on the right). For example, the BPM of X_4 presented a strong 5.64 ms peak, which was not observed for the BPM of $D^{2,3}X$. The negative mode was observed to have fewer peaks in the BPMs than the positive mode. This might be caused by fragmentation occurring in negative ionization mainly to one direction from reducing end towards non-reducing end.

To conclude, both the positive and negative ionization modes were suitable for fingerprinting because all tetrasaccharide isomers had different BPM profiles. Moreover, the results showed that BPMs can strengthen the MS/MS identification when isomeric fragment ions are formed. Since the used amount of collision energy has an impact on the fragmentation and formed MS/MS and BPM spectra the same collision energy should always be used. If there are any doubts, some diagnostic extracted ions from Tables 2 And 3 could be determined after fingerprinting to confirm the identification.

4. Conclusion

TWIMS-MS and CID-TWIMS-MS/MS were found to be promising methods for the structural analysis of isomeric XOS and AXOS oligosaccharides. Based on the presented TWIMS-MS and CID-TWIMS-MS/MS methods, we were able to differentiate between most of the isomeric structures of the studied (A)XOS. For TWIMS-MS, the best separation was achieved for positively charged $[M + Na]^+$ ions compared to negatively charged $[M-H]^-$ and $[M + Cl]^-$ ions. All four isomeric pentasaccharides were differentiated by TWIMS-MS as $[M + Na]^+$ precursor ions. The differentiation of isomeric trisaccharides required a comparison of the precursor ATDs from both positive and negative ionization modes. Three of the isomeric tetrasaccharide precursor ions had very similar ATDs and could not be separated by TWIMS-MS. Nonetheless, the tetrasaccharides could be identified by the BPMs and the MS/MS spectra produced by CID-TWIMS-MS/MS for both positive and negative ionization. By using the CID-TWIMS-MS/MS, we could also differentiate between most of the isomeric fragment ions from (A)XOS, e.g., the Ara-substituted fragment ions were differentiated from the linear xylan backbone XOS fragments; however, small disaccharide sized fragment ions could not be separated.

In this study, the samples were isolated fractions of oligosaccharides released from arabinoxylan. For the analysis of the isomeric oligosaccharides in mixtures, the implemented IM-MS method is recommended to be combined with the HILIC. In addition, to improve the method, some samples could be re-analyzed using ^{18}O-reducing end labelling to confirm the assumptions made regarding C- and Y-type fragments in CID-TWIMS-MS/MS. Of interest would also be to test the CID fragmentation after the IM separation to determine whether the IM separated fragment ions will produce linkage diagnostic ions.

CRediT authorship contribution statement

Minna Juvonen: Methodology, Investigation, Writing - original draft. **Edwin Bakx:** Resources, Writing - review & editing. **Henk Schols:** Resources, Writing - review & editing. **Maija Tenkanen:** Writing - review & editing, Supervision.

Declaration of Competing Interest

The authors declare that they have no known competing financial interests or personal relationships that could have appeared to influence the work reported in this paper.

Acknowledgements

Financial support from the Finnish Food Research Foundation and the Finnish Concordia Fund is gratefully acknowledged.

Appendix A. Supplementary data

Supplementary data to this article can be found online at https://doi.org/10.1016/j.foodchem.2021.130544.

References

Asam, M. R., & Glish, G. L. (1997). Tandem mass spectrometry of alkali cationized polysaccharides in a quadrupole ion trap. *Journal of the American Society for Mass Spectrometry, 8*(9), 987–995.

Both, P., Green, A. P., Gray, C. J., Šardzík, R., Voglmeir, J., Fontana, C., … Eyers, C. E. (2014). Discrimination of epimeric glycans and glycopeptides using IM-MS and its potential for carbohydrate sequencing. *Nature Chemistry, 6*(1), 65–74.

Clowers, B. H., Dwivedi, P., Steiner, W. E., Hill, H. H., & Bendiak, B. (2005). Separation of sodiated isobaric disaccharides and trisaccharides using electrospray ionization-atmospheric pressure ion mobility-time of flight mass spectrometry. *Journal of the American Society for Mass Spectrometry, 16*(5), 660–669.

Čmelík, R., & Chmelík, J. (2010). Structural analysis and differentiation of reducing and nonreducing neutral model starch oligosaccharides by negative-ion electrospray ionization ion-trap mass spectrometry. *International Journal of Mass Spectrometry, 291*(1-2), 33–40.

Domon, B., & Costello, C. E. (1988). A systematic nomenclature for carbohydrate fragmentations in FAB-MS/MS spectra of glycoconjugates. *Glycoconjugate Journal, 5*(4), 397–409.

Dwivedi, P., Bendiak, B., Clowers, B. H., & Hill, H. H. (2007). Rapid resolution of carbohydrate isomers by electrospray ionization ambient pressure ion mobility spectrometry-time-of-flight mass spectrometry (ESI-APIMS-TOFMS). *Journal of the American Society for Mass Spectrometry, 18*(7), 1163–1175.

Fauré, R., Courtin, C. M., Delcour, J. A., Dumon, C., Faulds, C. B., Fincher, G. B., … O'Donohue, M. J. (2009). A Brief and informationally rich naming system for oligosaccharide motifs of heteroxylans found in plant cell walls. *Australian Journal of Chemistry, 62*(6), 533. https://doi.org/10.1071/CH08458.

Fenn, L. S., & McLean, J. A. (2011). Structural resolution of carbohydrate positional and structural isomers based on gas-phase ion mobility-mass spectrometry. *Physical Chemistry Chemical Physics, 13*(6), 2196–2205.

Fukui, K., Kameyama, A., Mukai, Y., Takahashi, K., Ikeda, N., Akiyama, Y., & Narimatsu, H. (2006). A computational study of structure–reactivity relationships in Na-adduct oligosaccharides in collision-induced dissociation reactions. *Carbohydrate Research, 341*(5), 624–633.

Gabelica, V., & Marklund, E. (2018). Fundamentals of ion mobility spectrometry. *Current Opinion in Chemical Biology, 42*, 51–59.

Gabryelski, W., & Froese, K. L. (2003). Rapid and sensitive differentiation of anomers, linkage, and position isomers of disaccharides using High-Field Asymmetric Waveform Ion Mobility Spectrometry (FAIMS). *Journal of the American Society for Mass Spectrometry, 14*(3), 265–277.

Gaye, M. M., Kurulugama, R., & Clemmer, D. E. (2015). Investigating carbohydrate isomers by IMS-CID-IMS-MS: Precursor and fragment ion cross-sections. *Analyst, 140*(20), 6922–6932.

Harvey, D. (2005). Fragmentation of negative ions from carbohydrates: Part 1. Use of nitrate and other anionic adducts for the production of negative ion electrospray spectra from N-linked carbohydrates. *Journal of the American Society for Mass Spectrometry, 16*(5), 622–630.

Harvey, D. J., Scarff, C. A., Edgeworth, M., Crispin, M., Scanlan, C. N., Sobott, F., … Scrivens, J. H. (2013). Travelling wave ion mobility and negative ion fragmentation for the structural determination of N-linked glycans. *Electrophoresis, 34*(16), 2368–2378.

Hofmann, J., Struwe, W. B., Scarff, C. A., Scrivens, J. H., Harvey, D. J., & Pagel, K. (2014). Estimating collision cross sections of negatively charged N-glycans using traveling wave ion mobility-mass spectrometry. *Analytical Chemistry, 86*(21), 10789–10795.

Hofmann, J., Hahm, H. S., Seeberger, P. H., & Pagel, K. (2015). Identification of carbohydrate anomers using ion mobility-mass spectrometry. *Nature, 526*(7572), 241–244.

Hofmann, J., Stuckmann, A., Crispin, M., Harvey, D. J., Pagel, K., & Struwe, W. B. (2017). Identification of Lewis and blood group carbohydrate epitopes by ion mobility-tandem-mass spectrometry fingerprinting. *Analytical Chemistry, 89*(4), 2318–2325.

Hofmeister, G. E., Zhou, Z., & Leary, J. A. (1991). Linkage position determination in lithium-cationized disaccharides- tandem mass-spectrometry and semiempirical calculations. *Journal of the American Chemical Society, 113*(16), 5964–5970.

Juvonen, M., Kotiranta, M., Jokela, J., Tuomainen, P., & Tenkanen, M. (2019). Identification and structural analysis of cereal arabinoxylan-derived oligosaccharides by negative ionization HILIC-MS/MS. *Food Chemistry, 275*, 176–185.

Leijdekkers, A. G. M., Huang, J.-H., Bakx, E. J., Gruppen, H., & Schols, H. A. (2015). Identification of novel isomeric pectic oligosaccharides using hydrophilic interaction chromatography coupled to traveling-wave ion mobility mass spectrometry. *Carbohydrate Research, 404*, 1–8.

Körner, R., Limberg, G., Christensen, T. M. I. E., Mikkelsen, J. D., & Roepstorff, P. (1999). Sequencing of partially methyl-esterified oligogalacturonates by tandem mass spectrometry and its use to determine pectinase specificities. *Analytical Chemistry, 71*(7), 1421–1427.

Maina, N. H., Juvonen, M., Domingues, R. M., Virkki, L., Jokela, J., & Tenkanen, M. (2013). Structural analysis of linear mixed-linkage glucooligosaccharides by tandem mass spectrometry. *Food Chemistry, 136*(3-4), 1496–1507.

Pagel, K., & Harvey, D. J. (2013). Ion mobility-mass spectrometry of complex carbohydrates: Collision cross sections of sodiated N-linked glycans. *Analytical Chemistry., 85*(10), 5138–5145.

Pastell, H., Virkki, L., Harju, E., Tuomainen, P., & Tenkanen, M. (2009). Presence of 1→3-linked 2-O-β-D-xylopyranosyl-α-L-arabinofuranosyl side chains in cereal arabinoxylans. *Carbohydrate Research, 344*(18), 2480–2488.

Pastell, H., Tuomainen, P., Virkki, L., & Tenkanen, M. (2008). Step-wise enzymatic preparation and structural characterization of singly and doubly substituted arabinoxylo-oligosaccharides with non-reducing end terminal branches. *Carbohydrate Research, 343*(18), 3049–3057.

Pfenninger, A., Karas, M., Finke, B., & Stahl, B. (2002). Structural analysis of underivatized neutral human milk oligosaccharides in the negative ion mode by nano-electrospray MS n (Part 1: Methodology). *Journal of the American Society for Mass Spectrometry, 13*(11), 1331–1340.

Quéméner, B., Ordaz-Ortiz, J. J., & Saulnier, L. (2006). Structural characterization of underivatized arabino-xylo-oligosaccharides by negative-ion electrospray mass spectrometry. *Carbohydrate Research, 341*(11), 1834–1847.

Rantanen, H., Virkki, L., Tuomainen, P., Kabel, M., Schols, H., & Tenkanen, M. (2007). Preparation of arabinoxylobiose from rye xylan using family 10 *Aspergillus aculeatus* endo-1,4-β-D-xylanase. *Carbohydrate Polymers, 68*(2), 350–359.

Struwe, W. B., Baldauf, C., Hofmann, J., Rudd, P. M., & Pagel, K. (2016). Ion mobility separation of deprotonated oligosaccharide isomers – evidence for gas-phase charge migration. *Chemical Communications, 52*(83), 12353–12356.

Yamagaki, T., & Sato, A. (2009). Isomeric oligosaccharides analyses using negative-ion electrospray ionization ion mobility spectrometry combined with collision-induced dissociation MS/MS. *Analytical Sciences: The International Journal of the Japan Society for Analytical Chemistry, 25*(8), 985–988.

Zhu, M., Bendiak, B., Clowers, B., & Hill, H. H. (2009). Ion mobility-mass spectrometry analysis of isomeric carbohydrate precursor ions. *Analytical and Bioanalytical Chemistry, 394*(7), 1853–1867.